GAMMA RADIATION EFFECTS ON THE ELECTRICAL CONDUCTIVITY OF PYROLYTIC BORON NITRIDE

by

Dean Clifford Jones

A Thesis Submitted to the
Graduate Faculty in Partial Fulfillment of
The Requirements for the Degree of
MASTER OF SCIENCE

Major Subject: Nuclear Engineering

Iowa State University
Ames, Iowa

1969

TABLE OF CONTENTS

INTRODUCTION

Pyrolytic boron nitride is a relatively new form of boron nitride. It was first produced in the United States about 1964 by Union Carbide Corporation (1). This new material is finding many useful applications and its unique properties are providing solutions to many heretofore unsolved problems.

Two specific properties of pyrolytic boron nitride finding usefulness in electronics applications are those of high electrical resistivity and high dielectric strength. Work has been done by Westinghouse (2) using pyrolytic boron nitride as the dielectric for high temperature capacitors. The value of pyrolytic boron nitride in this application is evident from the comparative data in the reference (2). These data suggest that it is now possible to produce capacitors that will function adequately at temperatures up to 1100° F, as compared to the previous limitation of approximately 750° F. In electronics this is a most significant advancement since most other major electronic components such as semiconductors, vacuum tubes, and resistors have already been developed which can operate at temperatures up to 1000° F. Hence, in the past the capacitor has been a major limiting component in the development of high temperature electronic devices. The discovery of pyrolytic boron nitride appears to hold the solution to this problem.

For the nuclear engineer, the logical extension of this development is to question the behavior of this new material in a radiation environment such as that encountered in space or in close proximity to a nuclear reactor. Following the current development of compact nuclear reactors for space deployment, a need might be expected to arise for a high temperature capacitor with low electrical losses under intense irradiation. Based on the remarkable performance of pyrolytic boron nitride capacitors in an unirradiated environment, this material logically becomes a prime candidate for this application.

To begin the determination of the suitability of pyrolytic boron nitride for the application discussed, an investigation of the effects of gamma radiation on the electrical conductivity of pyrolytic boron nitride was proposed. Such work would provide an indication on the advisability of further investigations of electrical properties of pyrolytic boron nitride in a radiation environment.

With these considerations in mind an investigation was undertaken to determine the effects of Co^{60} gamma radiation on the electrical conductivity of pyrolytic boron nitride.

CONDUCTIVITY IN PYROLYTIC BORON NITRIDE

Background

Pyrolytic boron nitride can be produced by introducing boron trichloride and ammonia into a deposition chamber at 1 mm Hg and 3450° F. Under these conditions a highly pure boron nitride, called pyrolytic boron nitride, crystallizes on a graphite substrate.

$$BCl_3 + NH_3 \xrightarrow[1 \text{ mm Hg}]{3450^\circ \text{ F}} BN + 3HCl$$

The crystals formed in this manner are hexagonal, with lattice parameters oriented as indicated in Figure 1.

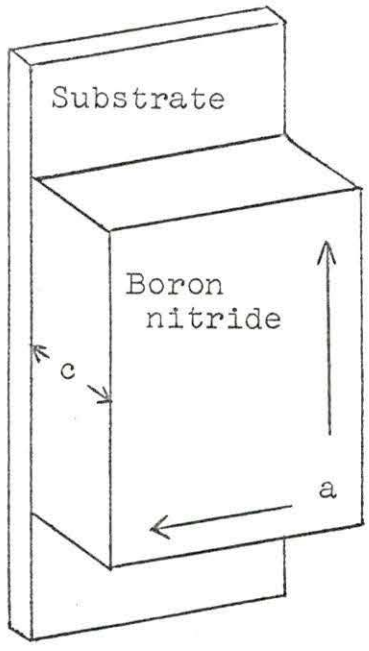

Figure 1. Lattice orientation in pyrolytic boron nitride

In the process developed by Union Carbide (1, 3) pyrolytic boron nitride is produced with total impurities less than 100 ppm and with a crystallite orientation of 1000:1. Pyrolytic boron nitride is anisotropic with respect to many of its properties, including that of resistivity.

Pyrolytic boron nitride exhibits many favorable properties, in addition to those already indicated, which make it particularly attractive for high temperature electrical application. It is machinable much like phenolic plastics, although this investigator learned that it flakes easily along the "a" lattice direction. Pyrolytic boron nitride sublimes at 5432° F and exhibits an oxidation rate that is negligible up to 1400° F, approximately 0.1 mg/cm^2-min at 2600° F and approximately 8.0 mg/cm^2-min at 3600° F. It is chemically inert to most substances up to 2000° F; and it has a dielectric strength of 4000 volts/mil at room temperature.

Dark Conductivity in Pyrolytic Boron Nitride

The conductivity, σ , of a material is given by

$$\sigma = \sum_{j=1}^{m} n_j q_j \mu_j \qquad (1)$$

where n_j is the concentration of carriers of the jth type, q_j is the charge of the jth type carrier and μ_j is the mobility of the jth type carrier.

There are several classifications of mechanisms, depending on the type of carriers, by which electricity is conducted in ceramic materials. Five principal classifications are listed below (4):

Cation-cationic--Conduction is by mobile cations where motion of the ion-carrier is in one direction only.

Anion-cationic--Conduction is by mobile positive and negative ion-carriers.

Electron-cationic--Conduction is by cations which emanate from the anode. An electron travels from the cathode and reduces the cation in the material.

Electron-anionic--Conduction is by the motion of anions which are liberated at the anode or in lattice defects and are neutralized to become atoms and defect centers.

Purely electronic--Conduction is by electrons traveling in one direction while an equal number of "holes" move in the opposite direction.

Bogoroditskii (4) reports that conduction in unirradiated boron nitride is "purely electronic". This can be confirmed experimentally by observing whether or not "electrochemical aging" occurs. In the case of "purely electronic" conduction no aging will occur. Electronic conduction is characteristic of materials with atomic lattices such as that of boron nitride (4).

The purity of electronic conduction in any material depends of course on the degree of the chemical purity.

Understandably the introduction of impurities into a material such as boron nitride may increase its electrical conductivity by introducing other conduction mechanisms. It is therefore possible for a sample of boron nitride containing impurities to exhibit electronic conduction plus one or more of the other four conduction mechanisms. It is in fact the presence of impurities in semiconductor materials that contribute to their unique electrical properties (5, 6, 7, 8, 9). Since the conductivity in semiconductors applies equally to insulators (10), much of the discussion to follow is taken from publications on semiconductors.

In the case of pure electronic conduction Equation 1 becomes

$$\sigma = n_e e u_e + n_h e u_h \qquad (2)$$

where n_e and n_h refer to concentrations of "free" electrons and "holes" respectively, e is the charge of an electron, u_h and u_e refer to the mobilities of the "holes" and "free" electrons respectively (9). A "free" electron is one which has been elevated to an energy state called the conduction band. Normally, electrons are elevated to the conduction band by thermal excitation. The conduction band is an energy state higher than the valence state separated by an energy gap. Figure 2 illustrates the relation of these energy states (6). Electrons in the conduction band are

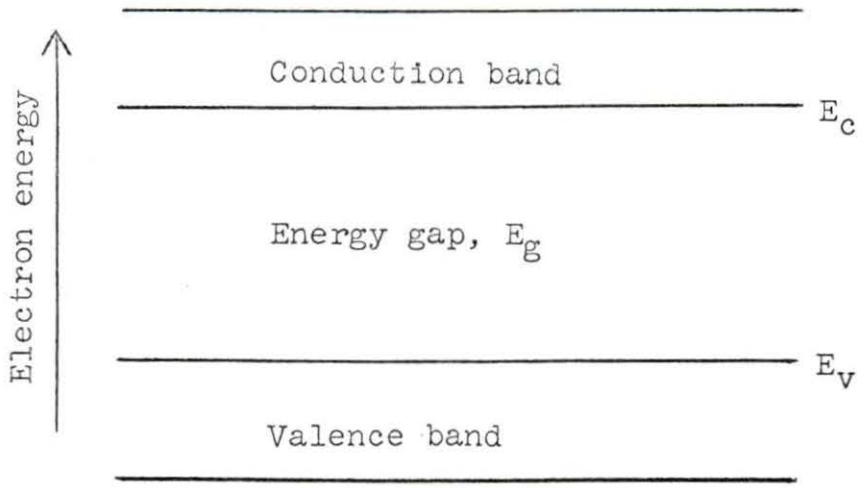

Figure 2. Electronic energy bands in an electronic conductor

considered to be free to serve as carriers of electricity. A "hole" is a positive site, the result of an electron deficiency created by the departure of an electron previously elevated to the conduction band. Both "hole" and "free" electron are considered to be carriers of electricity.

The concentration of "free" electrons and "holes" in a material is temperature dependent. In the case of intrinsic conductivity, i.e., conductivity attributable to the pure material, n_e and n_h are equal. An expression for n_e and n_h is given by (8)

$$n_e = n_h = 2 \left(\frac{2\pi kT}{h^2} \right)^{3/2} (m_e m_h)^{3/4} e^{-E_g/2kT} \qquad (3)$$

where k is Boltzmann's constant, h is Planck's constant, m_e and m_h are the effective masses of electrons and "holes", E_g is the energy gap and T is the temperature in degrees Kelvin.

Combining Equation 3 with 2 yields

$$\sigma_i = 2|e|\left(\frac{2\pi kT}{h^2}\right)^{3/2} (m_e m_h)^{3/4}\, e^{-E_g/2kT}\, (u_e + u_h) \tag{4}$$

where σ_i refers to intrinsic conductivity. The mobilities, u_e and u_h, are also temperature dependent. In the case of atomic lattices, which applies to boron nitride, the mobility varies as $T^{-3/2}$ according to Ioffe (7).

$$u_e + u_h = MT^{-3/2} + NT^{-3/2} = PT^{-3/2} \tag{5}$$

M, N, and P are constants with P = M + N.

Combining Equations 4 and 5, noting that the terms $T^{-3/2}$ and $T^{+3/2}$ cancel, and combining and redefining constants yields the expression

$$\sigma_i = Ae^{-B/T} \tag{6}$$

where A and B are constants. Extrinsic conductivity, σ_e, is that conductivity resulting from the presence of impurities or imperfections in a material. Thus, the total conductivity of a material with extrinsic conductivity is given by

$$\sigma = \sigma_i + \sigma_e \tag{7}$$

An expression for σ_e can be derived which is similar to that for σ_i, leading to the expression of the form (7)

$$\sigma_e = Ce^{-D/T} \tag{8}$$

where C and D are constants.

Combining Equations 6 and 8 yields an expression for the total conductivity without irradiation

$$\sigma = Ae^{-B/T} + Ce^{-D/T} \tag{9}$$

For materials whose conductivity varies according to Equation 9 a plot of $\ln\sigma$ versus $1/T$ yields a plot similar to Figure 3.

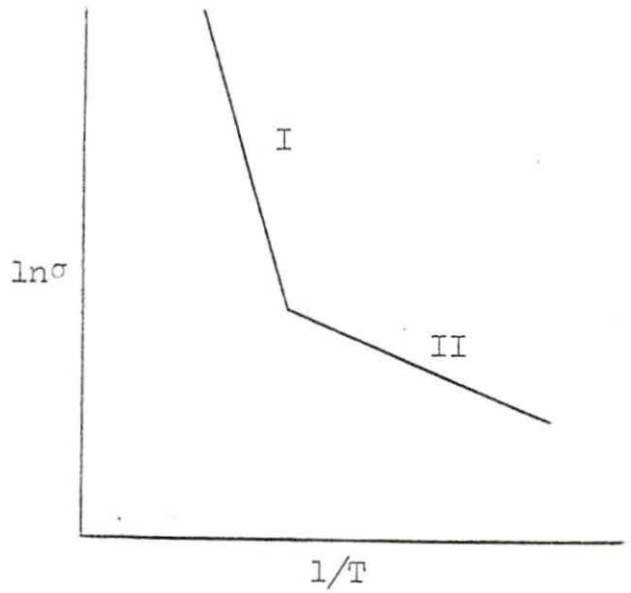

Figure 3. Intrinsic and extrinsic conductivity regions

The presence of two distinct straight lines in Figure 3 results from the differences in values of B and D in Equation 9. It is found that normally D is considerably less than B indicating that the first term dominates the plot in the high temperature region (region I) and the second term dominates in the low temperature region (region II). In other words, conductivity is predominately intrinsic at high temperatures and predominately extrinsic at low temperatures.

Radiation Induced Conductivity in Pyrolytic Boron Nitride

The effects of temperature, impurities, and imperfections on the conductivity of a material such as boron nitride in an unirradiated environment has been discussed in the previous section and can be expressed by Equation 9. Introducing a material such as boron nitride into a gamma radiation field introduces an additional source of carriers of electricity. On the basis of work reported by Vul (11) it is postulated that conductivity resulting from irradiation may be expressed by

$$\sigma_{ir} = G(\gamma)t^{n}e^{-F/T} \qquad (10)$$

where $G(\gamma)$ is a dose rate factor, F and n are constants, and t is irradiation time.

An expression for total conductivity in a radiation

field is obtained by combining Equations 9 and 10.

$$\sigma = Ae^{-B/T} + Ce^{-D/T} + G(\gamma)t^{n}e^{-F/T} \qquad (11)$$

As already indicated conductivity in pyrolytic boron nitride is electronic. The availability of electrons in the conduction band in the absence of radiation can be considered to result from thermal excitation of electrons in valence bands. The introduction of gamma radiation provides an additional source of free electrons to serve as carriers. Three principal mechanisms by which gamma radiation is absorbed in materials are the photoelectric effect, the Compton effect, and pair production (10, 12).

In the photoelectric effect a gamma photon interacts with an orbital electron in such a way that the whole of the photon energy, less the binding energy of the electron, is transferred to kinetic energy of the electron.

The Compton effect results when a photon transfers part of its energy to an electron as kinetic energy with the remaining energy being re-emitted as a lower energy gamma photon.

Pair production results when a photon of sufficiently high energy transforms into a positron and a negatron in the vicinity of an atomic nucleus. Photon energy in excess of 1.02 Mev is divided between the two particles as kinetic energy.

Each of the three mechanisms produces free electrons that could serve as carriers; however, the predominant mechanisms for the gamma energy spectrum of Co^{60} are the Compton and photoelectric effects (10, 12) since the Co^{60} gamma energies are 1.17 and 1.33 Mev.

It has been reported that the absorption of gamma radiation in pyrolytic boron nitride produces F centers much as occurs in alkali halides (13, 14). An F center in pyrolytic boron nitride is a positively charged nitrogen vacancy which has captured an electron as shown in Figure 4.

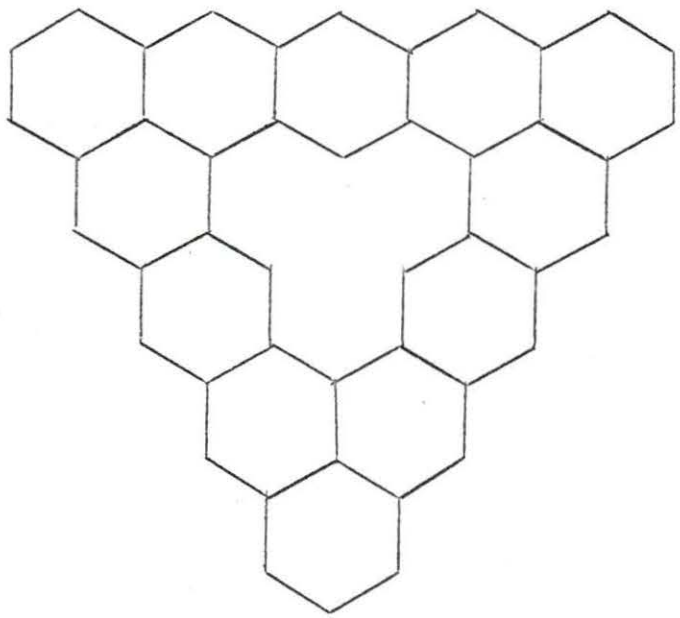

Figure 4. Nitrogen vacancy in boron nitride

It is reasonable to expect that production of these F centers will affect the conductivity of pyrolytic boron nitride and will be exhibited as time dependent conductivity. In the work reported (13) the gamma dose used was 1.5 x 10^8 R. In this experimental thesis time dependency was investigated up to a much smaller dose since the maximum dose rate available is less than 10^6 rad/hr.

The dose rate dependency is shown in Equation 10 by the parameter $G(\gamma)$. This parameter is a function of the number of electrons liberated by irradiation, n_{ir}, and the mobility of the liberated electrons, u_{ir}.

$$G(\gamma) \alpha n_{ir} u_{ir} \tag{12}$$

For a slab sample of thickness x, n_{ir} can be determined by the relation (15)

$$n_{ir} = \phi(o) M(1-e^{-\lambda x}) \tag{13}$$

where $\phi(o)$ is gamma flux, M is the number of secondary electrons produced, and λ is the absorption coefficient of the material. The thickness of the sample used in this investigation is so small compared to the half-thickness for gamma absorption that Equation 13 can be simplified to:

$$n_{ir} = \phi(o) M\lambda x \tag{14}$$

since e^{-x} expands by Taylor series to approximately 1-x when

$x << 1$. Equation 14 indicates that there is no significant flux depression in the sample and therefore electron liberation is uniform throughout the sample. Thus, since dose rate is proportional to flux,

$$n_{ir} \propto R \tag{15}$$

where R represents dose rate.

Vul (11) reports an approximate linear relation of dose rate to conductivity; however, should the production by radiation of electron "traps" significantly alter the total concentration of "traps", mobility might be expressed by a power of the dose rate, such as

$$u_{ir} = sR^b \tag{16}$$

where s and b are constants.

Then, at a constant temperature and steady state, Equation 10 becomes

$$\sigma_{ir} = rG(\gamma) = aR^c \tag{17}$$

where a, r, and c are constants.

Equation 11 becomes

$$\sigma = Ae^{-B/T} + Ce^{-D/T} + bR^c t n_e^{-F/T} \tag{18}$$

EXPERIMENTAL DISCUSSION

General

As mentioned previously, one purpose of investigating the electrical conductivity of pyrolytic boron nitride was to determine the value of this material for space applications. It is therefore desirable that conductivity measurements be made in a radiation field as near as possible to that of actual space radiation. Electron, proton and bremsstrahlung radiation constitute the three types of radiation that are of primary concern for space-electronic applications (12). In space maximum electron energies range from 1 to 5 Mev and proton energies range from 20 to several hundred Mev. The maximum energy of bremsstrahlung radiation is dependent upon that of the primary electron producing the radiation. With a tolerable amount of shielding electronic components could be shielded from electrons and low energy protons. For the purposes of this investigation it will be assumed that the space environment of concern is one where the electronic components are shielded from all electrons and protons and that bremsstrahlung (gamma) radiation is the only radiation of concern.

The Battelle Memorial Institute reports (12) that gamma radiation from Cobalt-60 sources provides a reasonable approximation of the effects to be expected from "5-Mev" bremsstrahlung radiation. Therefore, a Cobalt-60 source of

approximately 5000 curies was used to perform this investigation. A description of the source facility is given later in detail.

Apparatus and Equipment Restrictions

Design of the measuring apparatus and selection of associated equipment was dependent on a number of restrictive conditions which had to be provided for reliable conductivity measurements.

Magnitude of conductivity

There is no information available on the electrical conductivity or resistivity of pyrolytic boron nitride below 1800° F. Figure 5 shows the resistivity of pyrolytic boron nitride for temperatures above 1800° F as reported by Union Carbide (3). Included in Figure 5 for comparison are resistivities for hot pressed boron nitride and fused alumina. A linear extrapolation of "c" direction resistivity (dotted line) suggests that resistivities of 10^{12} to 10^{14} ohm-cm may be expected for the unirradiated material in the temperature range 800° to 1400° F. On the basis of this extrapolation the conductivity measuring apparatus had to be designed to measure resistivities up to 10^{14} ohm-cm.

Low electrical leakage in equipment

To design an apparatus capable of measuring resistivities up to 10^{14} ohm-cm, required that electrical leakage

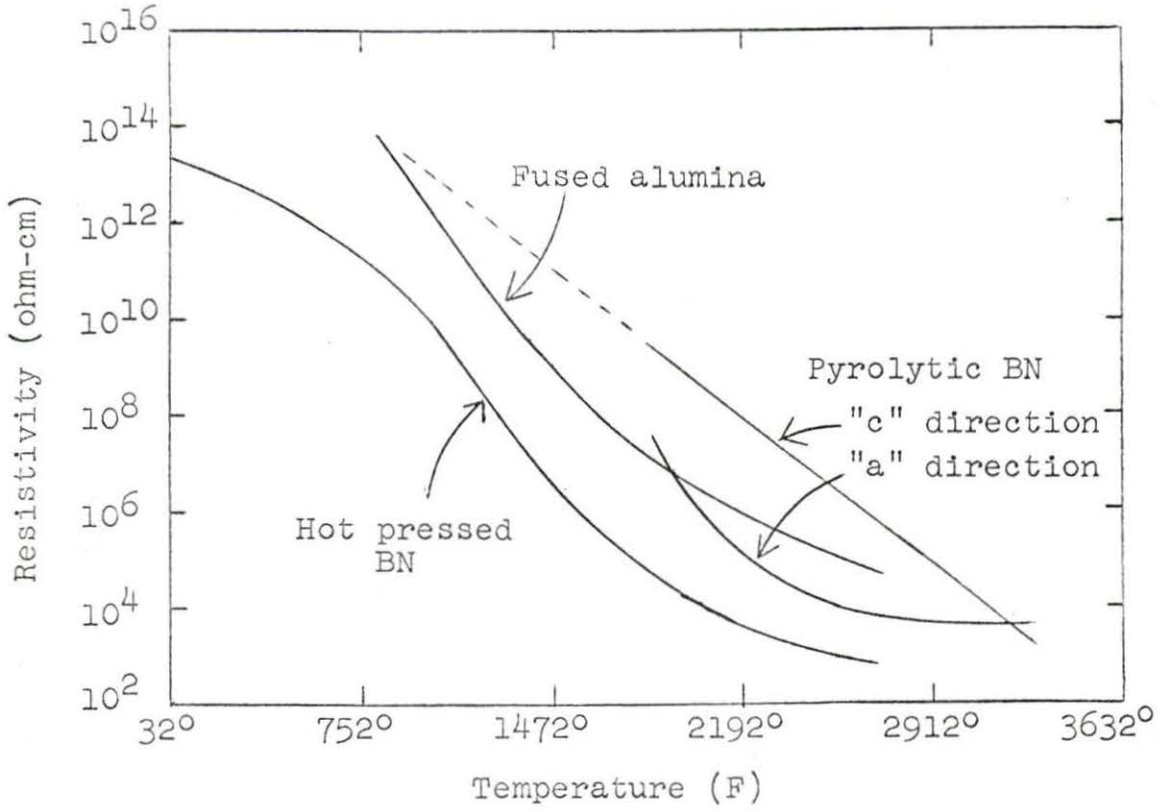

Figure 5. Electrical resistivities of boron nitride and alumina

across insulators at all terminals, junctions, feed-throughs, plugs, and jacks be of a minimum value. This restriction made careful selection of insulators and specimen supports mandatory.

High temperature capability

In line with work by Westinghouse (2) on high temperature capacitors with pyrolytic boron nitride as the dielec-

tric a temperature capability of at least 1100° F was selected. The completed apparatus had an upper limit of 1350° F, which proved to be fortunate since the temperature range of significance, with regard to irradiated behavior of pyrolytic boron nitride, was in the range 900° to 1300° F (480° to 700° C).

Measurement in vacuum

It was mandatory that conductivity measurements be conducted in a vacuum chamber for three important reasons.

The first reason was to protect the apparatus from excessive oxidation and to prevent burn-out of the heater coil when operating at upper temperature limits.

The second reason was to reduce to a minimum background conductivity attributable to gaseous conduction. Gaseous conduction was reported by Peters (16) as a significant problem in high temperature conductivity measurements of alumina. Since it was expected that pyrolytic boron nitride would have lower conductivity than alumina this problem becomes even more significant. Furthermore, gaseous conduction is greatly increased in a radiation field due to ionization effects. These effects can be reduced to a tolerable level by utilizing a vacuum system.

The third reason was to reduce electrical leakage due to surface conduction of samples and insulators. Moisture is the primary cause of surface conduction in most materials,

therefore, eliminating moisture from a material greatly increases its insulating ability. Alumina, which was selected for wide application in the apparatus is particularly susceptible to moisture-promoted surface conduction. Cohen reports (17) that removal of moisture from alumina at ambient pressures requires temperatures in excess of 1000° C and for this reason recommends vacuum operation to reduce surface conduction in alumina.

Based on the work of Dau and Davis (18) in measurements of electrical conductivity of alumina in a reactor environment, a vacuum upper limit of 25 microns was selected as a design objective.

Apparatus size

The single most restrictive and limiting requirement was that of apparatus size. The apparatus had to be constructed sufficiently small so that it could be inserted into the gamma irradiation facility. The overall maximum allowable dimensions of the apparatus was 4-1/4 inches in diameter and 15 inches in length. It was desirable that the diameter of the section containing the sample be less than 2 inches in order to achieve nearly the maximum gamma dose rate available in the facility. The end result of these restrictions was a limitation on sample size to less than 1/2 of an inch in diameter. Such a small sample is only marginally acceptable by standards set by the American Society for

Testing and Materials (19), which recommends that the diameter of the contact electrode be greater than four times the thickness of the sample. It will be shown later that this standard was just barely achievable.

Equipment Selection and Design

General

The basic conductivity measuring circuit selected for this work, shown in Figure 6, utilizes two unguarded electrodes. Preliminary tests were conducted using a guarded circuit (19) in which determination was made that surface conduction in pyrolytic boron nitride was negligible in the temperature range of concern. This information provided the basis for using an unguarded circuit.

Figure 7 shows a block diagram of the total system used for this research. Each component of the system is discussed in the following paragraphs.

Gamma irradiation facility

The gamma radiation source was provided by the gamma irradiation facility shown in Figure 8. This facility contains approximately 5000 curies of Cobalt-60 and is designed so that a test specimen mounted in the irradiation chamber (shown near the top center of the photo) can be lowered to a selected position in the center of a ring of six moveable stainless steel cans containing Cobalt-60.

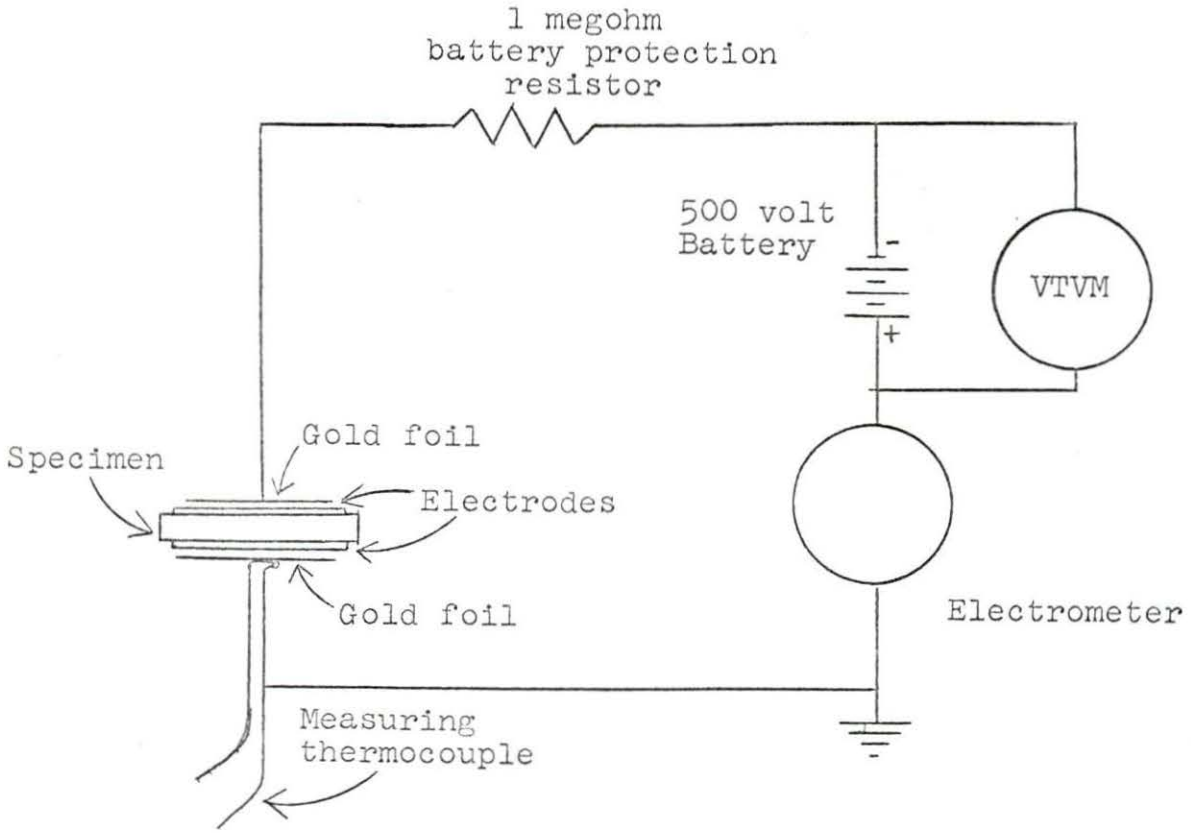

Figure 6. Conductivity measuring circuit

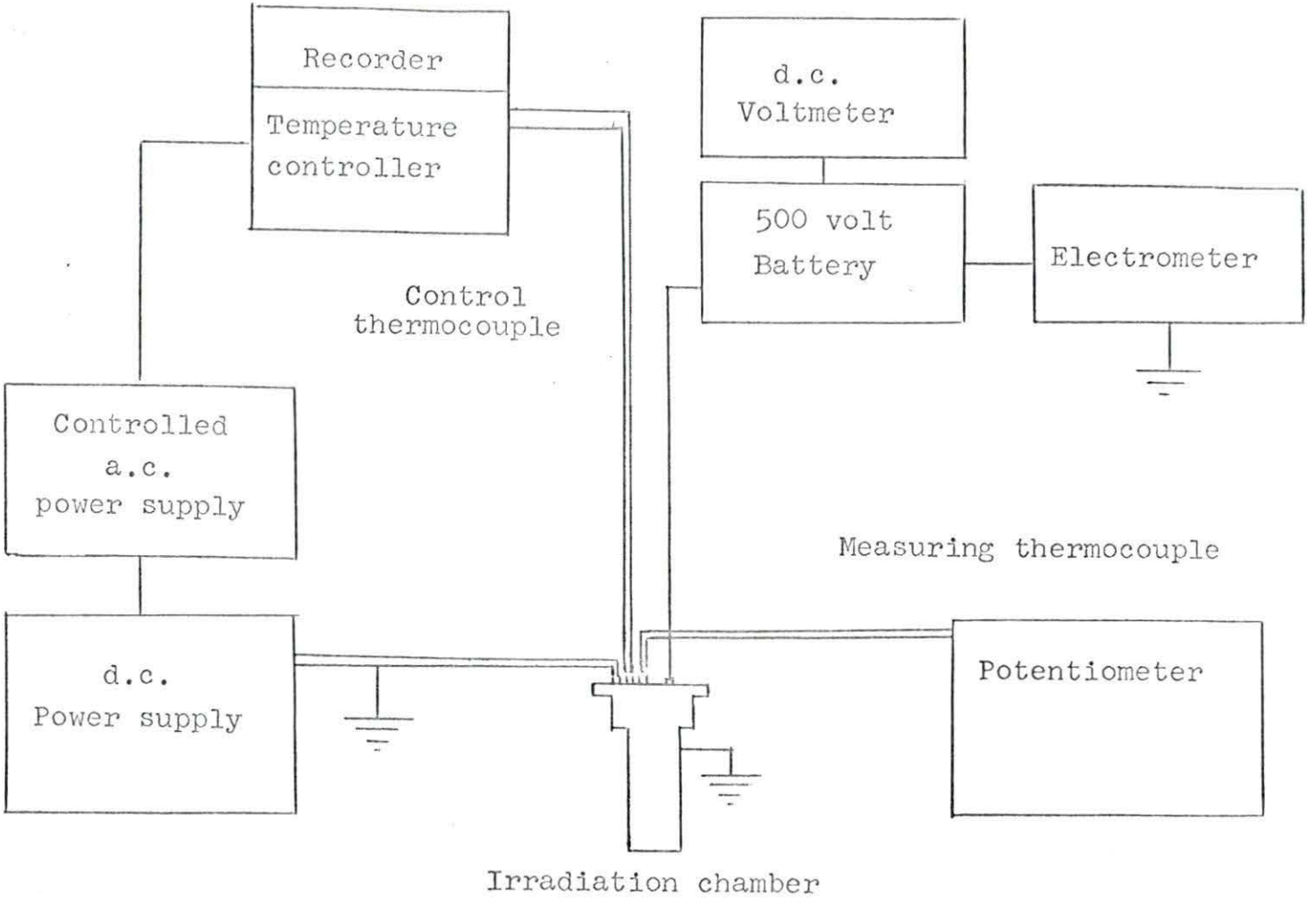

Figure 7. Block diagram of conductivity measuring equipment

Figure 8. Gamma irradiation facility

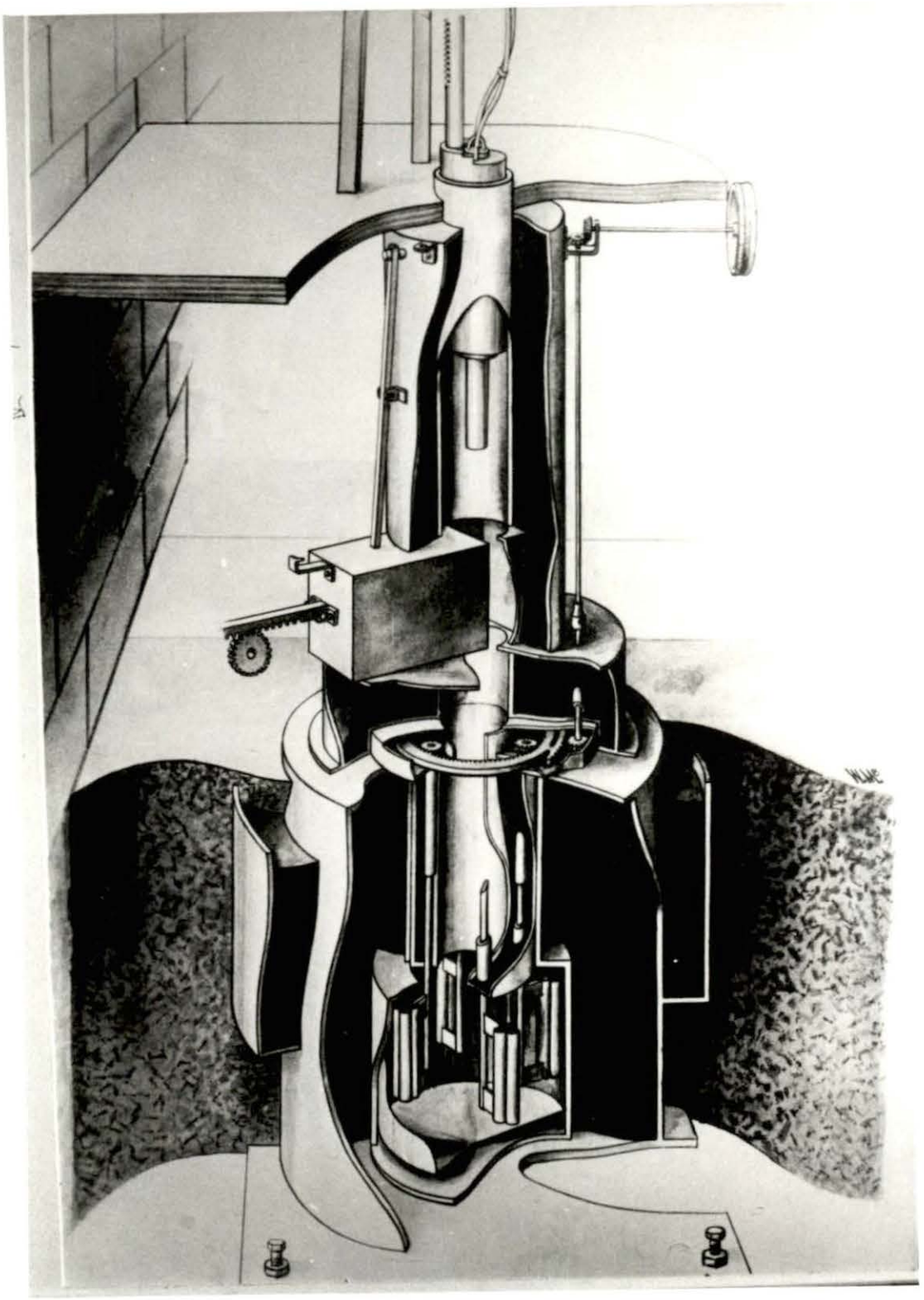

The dose rate received by the sample can be varied by rotating a hand-wheel (shown at top right of photo) which causes all of the cans of Cobalt-60 to rotate inward simultaneously. A maximum dose rate on the order of 10^4 rads/min can be achieved in the facility. Scales are provided for accurate verticle positioning of the specimen and horizontal positioning of the Cobalt-60 cans.

Measuring apparatus and vacuum irradiation chamber

Investigation of the gamma induced conductivity of sodium chloride by Carlson (20) using the gamma irradiation facility described above was performed using a tubular measuring apparatus in which the specimen was centered inside two concentric quartz tubes. Heat was provided by a nichrome heating element positioned between the two quartz tubes. The overall apparatus was approximately 1-5/8 inches in diameter and 4-7/8 inches in length and could be loaded into a slightly larger vacuum irradiation chamber. The chamber could be attached to the gamma facility and lowered into the gamma field. The design of this apparatus served as an initial guide for the design of an apparatus for the work of this thesis.

The measuring apparatus constructed for conductivity measurements of pyrolytic boron nitride is shown in Figure 9 and a photograph of the disassembled apparatus is shown in Figure 10. Based on the restriction demanding low

Figure 9. Conductivity measuring apparatus and vacuum irradiation chamber

1. Specimen
2. 5/16" O.D. alumina support tubes
3. Chromel-alumel measuring thermocouple
4. Pressed boron nitride brace
5. 1-3/18" diameter brass end plate
6. Pyrolytic boron nitride thermal masses
7. Chromel-alumel control thermocouple
8. Guard circuit lead support
9. 3/4" I.D. and 1" I.D. alumina tubes
10. Pyrolytic boron nitride insulators
11. Copper gasket
12. Cermaic feed-throughs (8)
13. Vacuum connector for 1/4" O.D. tubing
14. Teflon feed-through
15. Chamber mounting bracket
16. 1/4" bolt (10)
17. Pressure plate springs (3)
18. 1-3/8" brass pressure plate and end plate
19. 1/16" steel bolt (3)
20. 1/8" alumina "hot" lead guide
21. 21 gauge nichrome heater coil

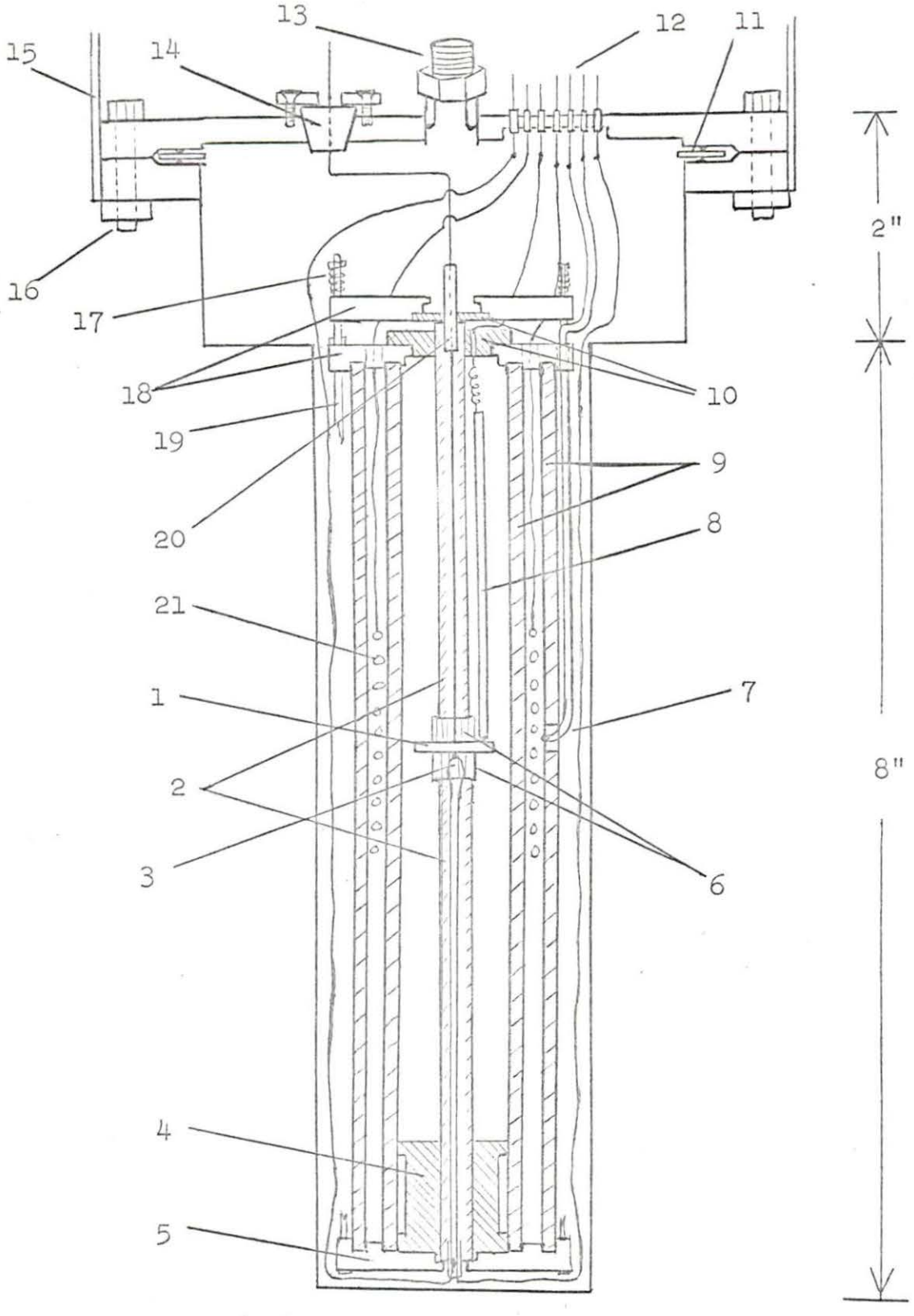
13
12
11
15
14
16
17
18
10
19
9
20
8
21
1
7
2
3
6
4
5
2"
8"

Figure 10. Partially disassembled conductivity measuring apparatus

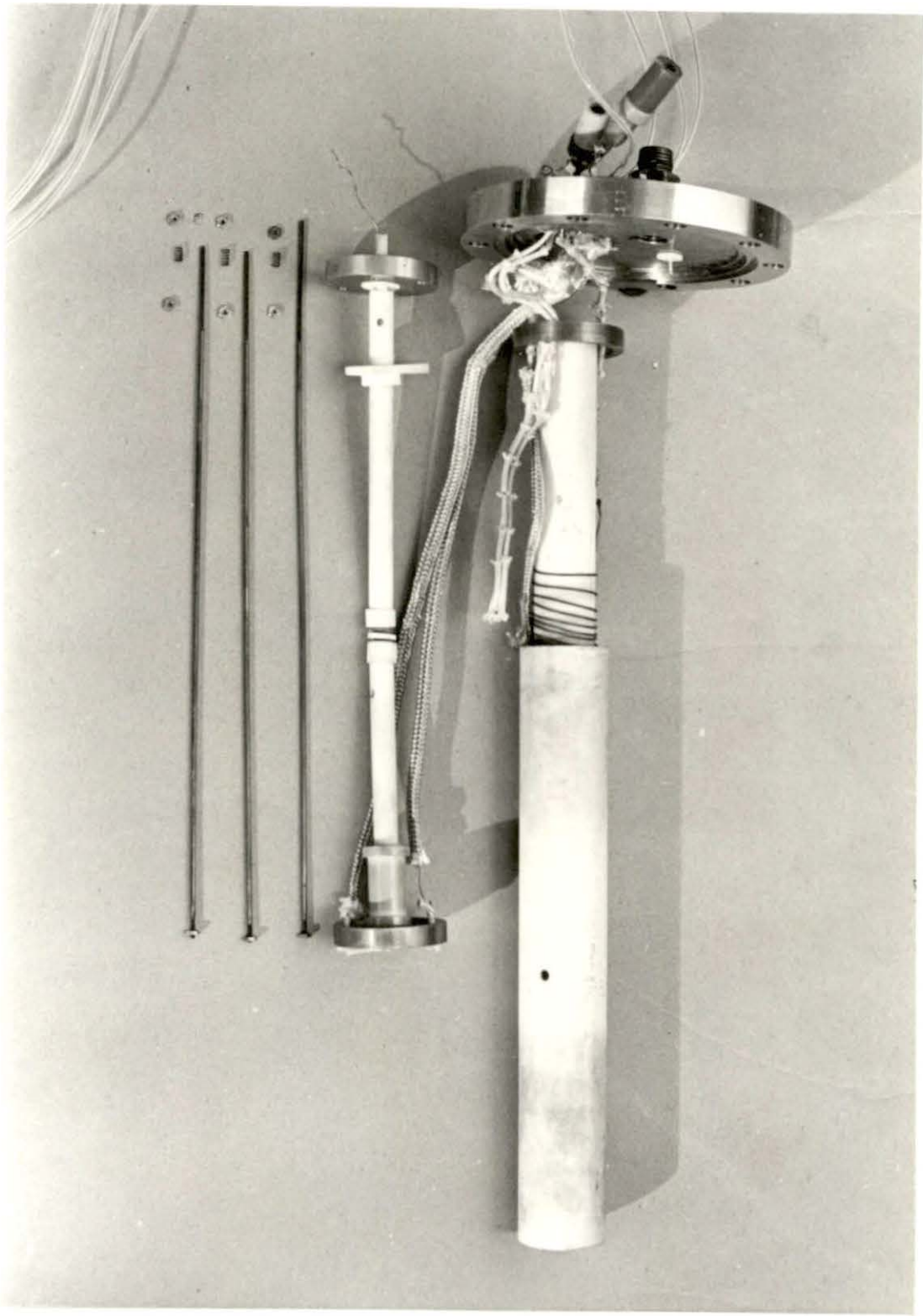

electrical leakage, 97 percent pure alumina tubing was selected as the basic insulating and support material in the apparatus. Alumina was selected because of its high thermal and electrical resistances. Values for resistivities of alumina at high temperatures, 1150° to 1450° F, have been reported ranging from 10^{12} ohm-cm (21) to 10^{9} ohm-cm (3) depending on experimental conditions and purity of alumina used. As temperature decreases the resistivity of alumina increases rapidly. Figure 5 shows a resistivity for alumina of 10^{14} ohm-cm at 752° F.

The high resistivity of alumina at relatively low temperatures was used to an advantage in the apparatus by using two small tubes of alumina to support the test specimen in the heated portion of the apparatus while supporting the tubes several inches from the heat source. Thus, the temperature of the support tubes will be much lower where they are supported than the test specimen and hopefully provide insulation of at least 10^{14} ohms between specimen and apparatus.

To provide additional assurance of electrical insulation for the test specimen two 1/4 inch thick disks of pyrolytic boron nitride were positioned on each side of the specimen. These parts served the additional function of acting as thermal masses, helping to stablize the temperature in the specimen. To further insulate the specimen the upper support tube was held at the cool end by two parts also made of pyrolytic boron nitride. The lower support tube was held

in place by a spool shaped part made of hot pressed boron nitride. With the upper support tube touching only the specimen and the two pyrolytic boron nitride supports, insulation of the specimen at a higher resistance than that of the specimen was guaranteed.

The heater coil was made of three feet of 21 gauge nichrome wire which permitted heating at 80 watts using a maximum of 16 volts d.c. and 5 amperes.

Two 28 gauge chromel-alumel thermocouples were used in the apparatus. One was positioned next to the heater coil to provide quick response for the temperature controller and the other was embedded in the lower 1/4 inch pyrolytic boron nitride disk supporting the specimen. The latter thermocouple served also as one of the leads in the measuring circuit.

The irradiation vacuum chamber, shown also in Figure 9, was fabricated of stainless steel, and was vacuum sealed by compressing a copper gasket between the upper and lower flanges of the chamber. The upper flange contained eight electrical feed-throughs with ceramic insulation, one specially designed teflon insulated feed-through, and a fitting for 1/4 inch copper tubing. The ceramic insulated feed-throughs were electrically insulated from the flange by a resistance greater than 10^{12} ohms. The teflon insulated feed-through had an electrical insulation better than 10^{15} ohms outside of the radiation field. Under the effects of

radiation the resistance of the teflon remained sufficiently high to be tolerable. Figure 11 illustrates the cross section of the teflon feed-through showing how a vacuum seal was obtained by compression of a tapered teflon insulator.

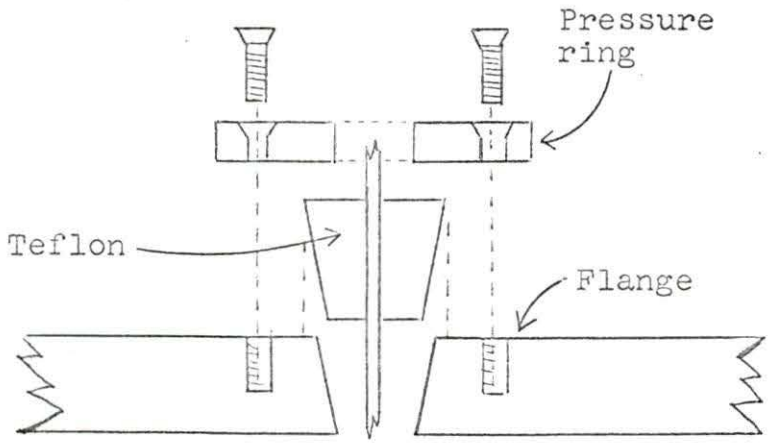

Figure 11. High resistance teflon feed-through

Radiation damage to the teflon insulation was expected to exceed tolerable limits after several hours of irradiation. Battelle (22) reports that mild to moderate damage occurs in teflon TFE after a gamma exposure of approximately 10^6 ergs/gm (approximately 10^4 rad). For this reason the feed-through was designed to permit frequent replacement. In actual use the first feed-through failed structurally after approximately 36 hours total irradiation time. The first indication of

damage to the teflon came when the feed-through failed to maintain an effective vacuum seal. The feed-through was checked before each use for unacceptable electrical leakage and structural damage. It was found that structurally damaged teflon behaves somewhat like soap and can be detected easily with a finger nail or the tip of a knife.

Electronic equipment

The battery shown in Figure 6 is a 510 volt low current Burgess Model U320 dry cell. A battery was selected rather than a filtered d.c. power supply to avoid problems of noise inherent in most filtered power supplies. The voltage selected was based on ASTM recommendations (19). The battery was suspended by teflon spaghetti inside a grounded aluminum box to exclude electronic noise. The body of the battery touched nothing other than the teflon spaghetti which was necessary to avoid electrical leakage through the skin of the battery.

The electrometer used to make current measurements was a Keithley Instrument Model 610B with a capability of measuring currents as low as 10^{-15} amperes with a one percent accuracy at full scale.

The battery voltage was monitored with a Hewlett-Packard model 412A d.c. vacuum tube voltmeter with an accuracy of ±10 volts at 500 volts.

The cables used in the measuring circuit were teflon insulated to assure low electrical leakage. Also, all electrical connectors used in the circuit were teflon insulated.

Vacuum system

The vacuum line to the irradiation chamber consisted of a combination of copper and rubber tubing with an intermediately positioned thermocouple vacuum gauge (Figure 12). The vacuum pump used was a Cenco Hyvac 14 with a 0.1 micron capability. The location of the vacuum gauge did not permit measurement of the absolute vacuum in the irradiation chamber, however, it was learned by experimentation that such measurement was not necessary and that satisfactory vacuum conditions could be achieved in the chamber by maintaining the vacuum at the gauge at approximately 10-15 microns. The validity of such procedure was established by making a series of background conductance measurements (measurements without a specimen in the chamber) to determine the vacuum reading at which background conductance was reasonably low and stable.

Temperature control system

As mentioned before one chromel-alumel thermocouple junction was positioned next to the heater coil for control by providing immediate sensing of temperature changes in the

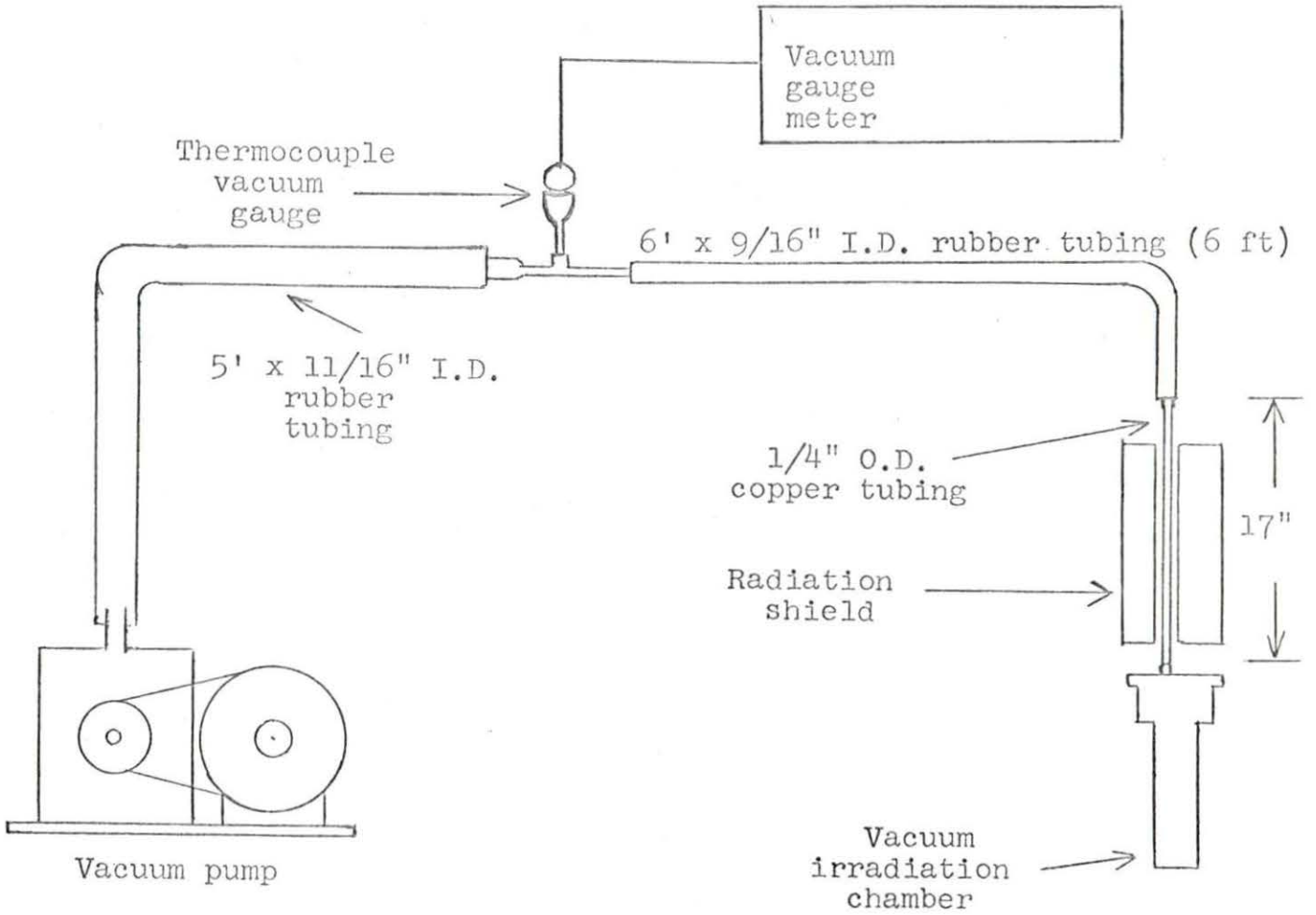

Figure 12. Vacuum system

apparatus. The signal from this thermocouple was fed into a Leeds and Northrup Series 80 C.A.T. controller and Speedomax H recorder. The output of the controller, in the form of a d.c. error voltage, was fed into a Leeds and Northrup universal silicon controlled rectifier power package which generated a controlled a.c. output. This fed into an Electro filtered d.c. power supply, model D-612T, which provided controlled power to the heater coils in the irradiation chamber. To use the control system one had only to set the desired temperature on the recorder.

Temperature read on the recorder was of course that temperature at the location of the thermocouple junction and not at the location of the specimen. To obtain the temperature of the specimen a second chromel-alumel thermocouple was used. The junction of this thermocouple was positioned in contact with the specimen as illustrated in Figure 9. The E.M.F. of this thermocouple was measured on a Honeywell Model 2745 potentiometer permitting accurate temperature conversion by use of thermocouple tables.

This completes the description of the equipment used to measure the conductivity of pyrolytic boron nitride. Photographs of the equipment are shown in Figures 13, 14, and 15.

Figure 13. Partially assembled irradiation chamber with conductivity apparatus assembled for background measurements

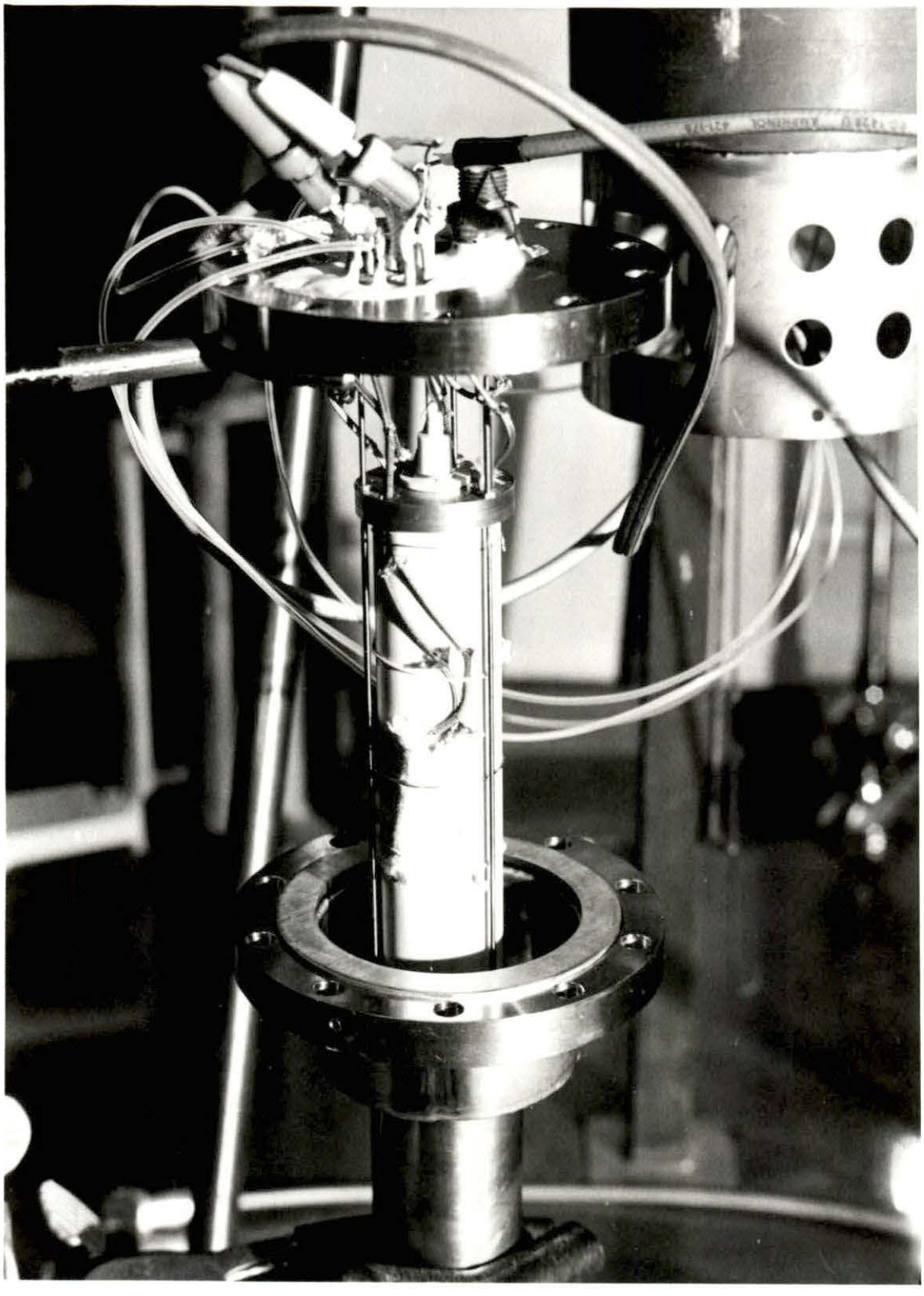

Figure 14. Completely assembled irradiation chamber mounted on gamma irradiation facility

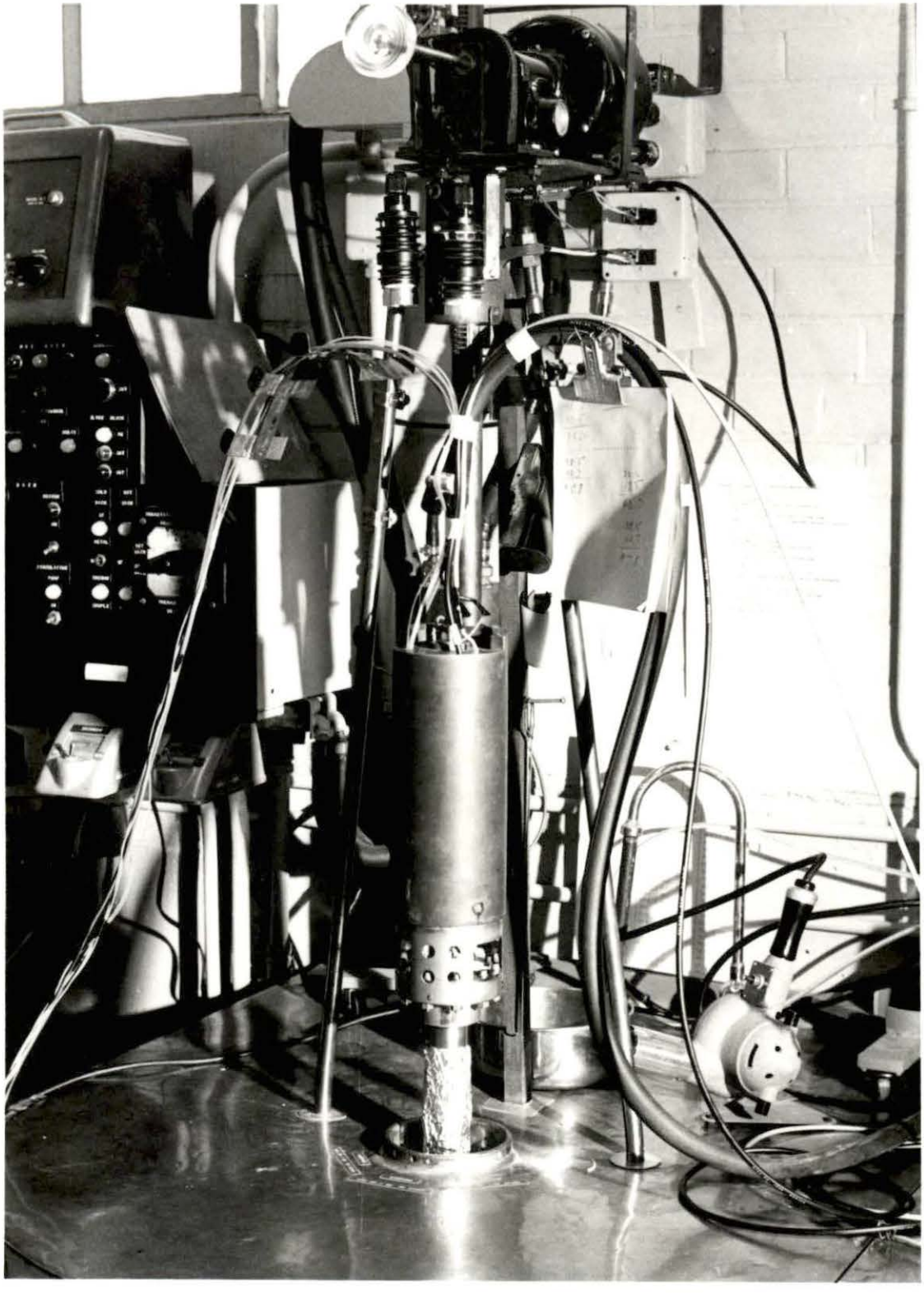

Figure 15. Complete experimental system including irradiation facility, temperature control and measuring instruments, conductivity measuring instruments, and vacuum system components


500 V

Experimental Procedures

Specimen preparation

Strips of 1/16 inch thick pyrolytic boron nitride were obtained from Union Carbide Corporation from which circular specimens were cut with a fine-toothed jewelers saw. The precise specimen thickness was measured with a micrometer to a 0.7 percent accuracy. Each sample was washed in acetone, methanol and water, and dried thoroughly at approximately 100° C before painting on the electrodes with silver electrode paint.

The electrodes were applied in the following steps:

1. Electrode No. 1 was painted on with a teflon brush.
2. The specimen was placed in a furnace with the unpainted side resting on another piece of pyrolytic boron nitride.
3. The specimen was baked for approximately 2 hours at 100° C, then 1 hour at 300° C, then 1/2 hour at 600° C and finally 1/4 hour at 700° C.
4. The specimen was then removed from the furnace, allowed to cool, and electrode No. 2 painted on.
5. Steps 2 and 3 were repeated with the previously painted side facing down.

The specimens were always handled with tweezers and carried and stored in dust free envelopes.

Equipment preparation

Prior to assembling the equipment with or without a specimen the following steps were taken:

1. The electrometer was turned on at least 24 hours before the intended time of data collection.
2. The upper alumina support tube, with associated pieces of boron nitride insulation, were thoroughly washed with acetone, methanol, and water and dried.
3. The inside and outside of the irradiation chamber, including top flange with insulated feed-throughs, were washed with acetone, methanol, and water.

The following were completed to prepare equipment for data collection:

1. The irradiation chamber was vacuum sealed for each use with a new copper gasket.
2. A 1/4 inch O.D. copper tube was attached to the chamber with a standard brass farrelled fitting and sealed with Glyptal.
3. After allowing 6 to 12 hours for the Glyptal to dry the vacuum pump was turned on, 12 watts power applied to the heater coil, and 12 to 36 hours allowed for degassing of the system. Degassing was considered complete when the vacuum gauge indicated 15 microns or less.

4. The measuring apparatus was heated once to its maximum temperature and cooled prior to taking data readings.
5. The measuring circuit battery was checked for proper voltage before, during and after each use.

Thermocouple calibration

Since temperatures obtained from thermocouple tables are based on ideal conditions it was necessary to calibrate the measuring thermocouple. This was accomplished by loading the conductivity measuring apparatus first with sample of aluminum and second with a sample of lead, each held in a small quartz cup. The quartz cup was placed in the position normally occupied by the boron nitride specimen. The apparatus was heated and cooled several times past the melting point of the metal. By observing the thermocouple output as the metal solidified, a constant E.M.F. was noted for a short period of time at the melting point of the metal. By following this procedure with two metals a reasonably accurate temperature correction was obtained which could be applied to all temperature measurements recorded. The correction obtained in this manner was $+31^{\circ}$ F for lead and $+29^{\circ}$ F for aluminum, for an average correction of 30° F. The aluminum used had a purity of 99.99 percent, the lead 99.999 percent.

Dose rate determination

All data taken in the irradiation facility were initially correlated to a source position indicator reading. This reading was taken from the hand wheel which is used to rotate the source cans inward. A method was required whereby the hand wheel could be converted to a corresponding dose rate. This was accomplished by replacing the specimen in the measuring apparatus with a vial of Fricke dosimetry solution and irradiating the vial at the desired hand wheel position for 60 seconds. The change in absorption coefficient of the Fricke solution, as determined with a Beckman DU spectrophotometer, permitted determination of the dose rate with an accuracy of ± 4 percent.

Data collection

Five types of data runs were made:

1. Background data--data taken with the complete system assembled without a specimen by varying temperature and dose rate.
2. Unirradiated specimen data--data taken by varying the temperature of specimen outside of the radiation field.
3. Irradiated specimen data--data taken by varying the temperature of specimen for each of three different dose rates.

4. Dose rate dependency data--data taken at a constant temperature with varying dose rate.
5. Time dependency data--data taken at a constant temperature and dose rate for a 30-minute time period.

In making data measurements careful attention had to be given to the relation of interacting resistances in the measuring circuit. Figure 16 illustrates the need for care by identifying each component of the circuit as a resistor.

Figure 16. Measuring circuit resistances

In Figure 16 R_s is specimen resistance, R_p is resistance of the battery protection resistor, R_b is the internal resistance of the battery and R_m is the loading resistor in the electrometer. An arbitrary requirement was made that R_p,

R_b and R_m introduce an error in the measured value of R_s no greater than one percent, thus requiring that

$$R_p + R_b + R_m \leq 100R_s$$

R_p was a 1 megohm resistor which could be ignored. Also the internal battery resistance could be assumed to be low enough to be negligible. Thus, in making measurements the input resistance to the electrometer was always maintained so that

$$R_m \leq 100R_s$$

Data processing

The assumption was made for the purpose of this work that ohms law is valid for all data taken. Then

$$R = E/I$$

where R is resistance, E voltage and I current.

Resistivity is defined by the following relation (19)

$$\rho = \frac{RA}{h}$$

Where A is cross sectional area of the specimen and h is the thickness of the specimen. The cross sectional area was determined by taking the average of the areas of the two electrodes on the specimen. Conductivity is simply the reciprocal of resistivity.

$$\sigma = \frac{1}{\rho}$$

After computing conductivity values, plots were made of $\ln\sigma$ versus $1/T$ and σ versus dose rate. From these plots the constants in Equation 18 were determined. The best straight line fit for the data plots were obtained by the method of least squares.

RESULTS AND DISCUSSION

General

The most significant and difficult problem that had to be overcome in this experiment was that of radiation induced electrical conductance of air, both inside and outside of the irradiation chamber. It was learned that air conductance inside the apparatus could be reduced to a relatively stable background by careful vacuum degassing as outlined in the previous section. Air conductance outside of the chamber was reduced to a tolerable level by complete shielding with teflon of that portion of the "hot" lead which was below the radiation shield. In radiation induced conductivity measurements, background conductance ranged from 1 percent to 46 percent of the total conductance depending on temperature and dose rate. Background conductance was found to be negligible in the absence of radiation in the temperature range of concern.

Three gamma radiation dose rates were used in this experiment. These rates, as determined by Fricke dosimetry, were 3.49×10^3 rad/min, 6.31×10^3 rad/min, and 1.35×10^4 rad/min.

The battery voltage remained at a constant 500 ± 10 volts throughout all data collection.

The data reported herein were taken with two specimens. Two separate runs were conducted with each specimen providing

a total of four sets of data for each dose rate. Specimen No. 1 measured 0.153 $\pm$ 0.001 cm in thickness and had an average electrode area of 0.506 $\pm$ .024 cm^2. Specimen No. 2 measured 0.153 $\pm$ .001 cm in thickness and had an average electrode area of 0.482 $\pm$ .027 cm^2.

Conductivity of Unirradiated Specimens

The conductivity of unirradiated pyrolytic boron nitride specimens used in this work is shown as a function of reciprocal temperature in Figure 17. The slope of this plot and the absence of a "knee" as shown in Figure 3 suggest that the data represent intrinsic conductivity only and that extrinsic conductivity is non-existent or insignificant over the temperature range of this investigation. This is probably due to the high purity of the specimens which limits the availability of extrinsic carriers. The difference in the plots of specimens 1 and 2 may be the result of contamination of one of the specimens or a systematic error in the temperature measurements between runs.

There was no detectable time dependency of the conductivity at 550° C over a period of 30 minutes, which suggests that the conduction mechanism in pyrolytic boron nitride is predominantly electronic as stated by Bogoroditskii (4).

The constants A and B in Equation 9 were determined from the composite plot in Figure 17 to be 1.99 x 10^3 $ohm^{-1}cm^{-1}$ and

Figure 17. Conductivity of unirradiated specimens

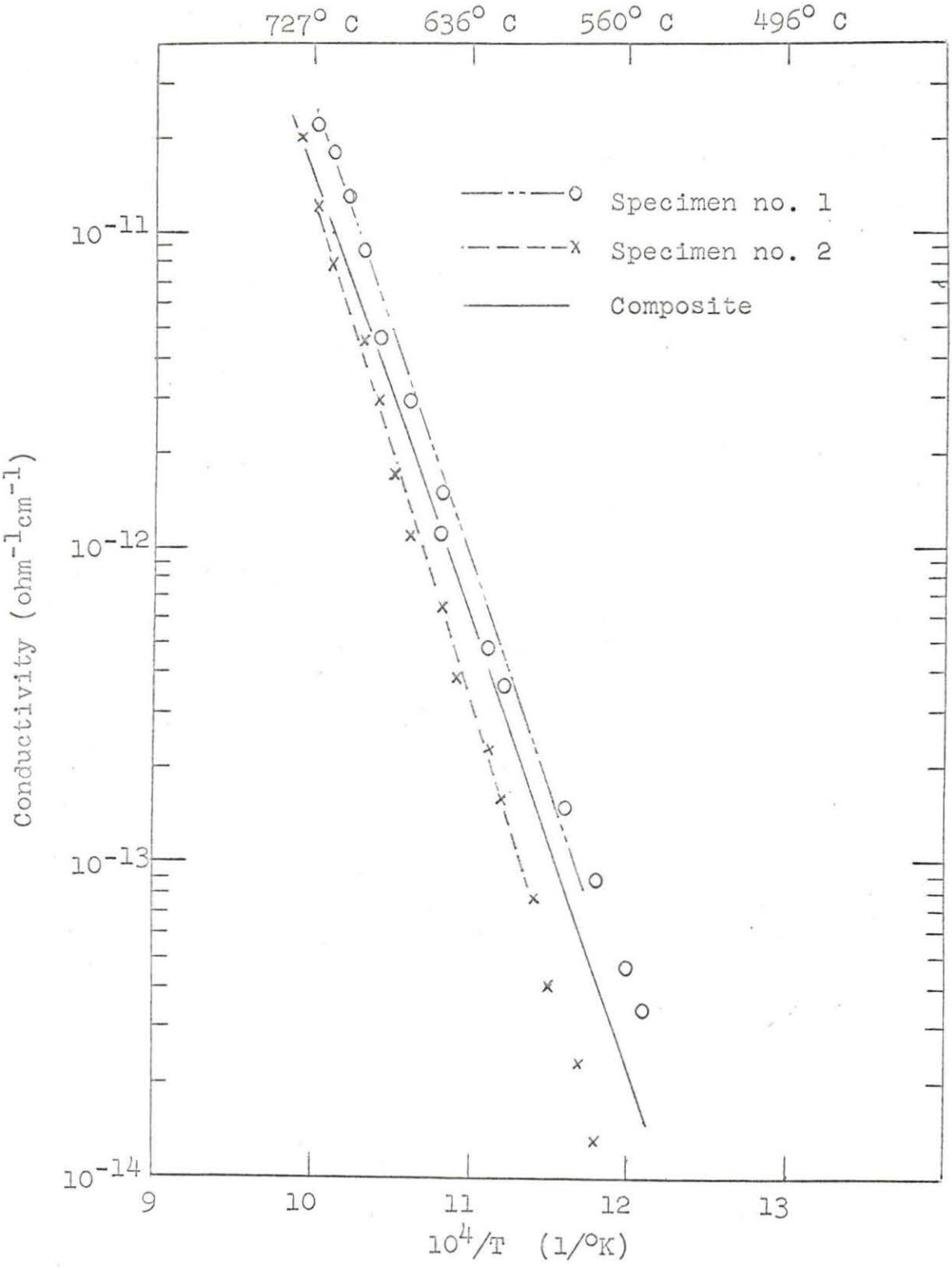
727° C
636° C
560° C
496° C
Specimen no. 1
Specimen no. 2
Composite
Conductivity (ohm^{-1}cm^{-1})
10^{-11}
10^{-12}
10^{-13}
10^{-14}
9
10
11
12
13
$10^4/T$ (1/°K)

3.26×10^4 °K respectively. The values of the constants C and D in Equation 9 cannot be determined from data obtained in this experiment, however, it can be said that their values are such that the second term in equation is rendered insignificant in the temperature range investigated. Thus, C can be considered to be approximately zero.

From the constant B the value of the energy gap or thermal activation energy, Eg, in Equation 4 is determined to be 5.62 ev since

$$B = \frac{Eg}{2k} \tag{19}$$

Conductivity in Irradiated Specimens

The conductivity of pyrolytic boron nitride under the influence of the gamma dose rate is shown as a function of reciprocal temperature in Figure 18. Also shown for comparison, without repeating data points, is the least squares fit of the data in Figure 17. It is noted that the effect of the radiation is to produce a two region plot such as appears in an unirradiated material which exhibits extrinsic conductivity as well as intrinsic conductivity. Just as in the case of extrinsic conductivity, gamma radiation induced conductivity is overshadowed by intrinsic conductivity above a certain dose rate dependent temperature. This is illustrated in Figure 18 by the fact that the conductivity of the specimen irradiated at 6.31×10^3 rad/min is essentially

Figure 18. Conductivity of gamma irradiated pyrolytic boron nitride

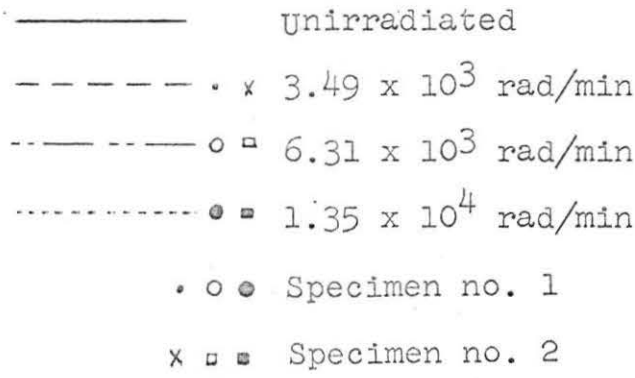

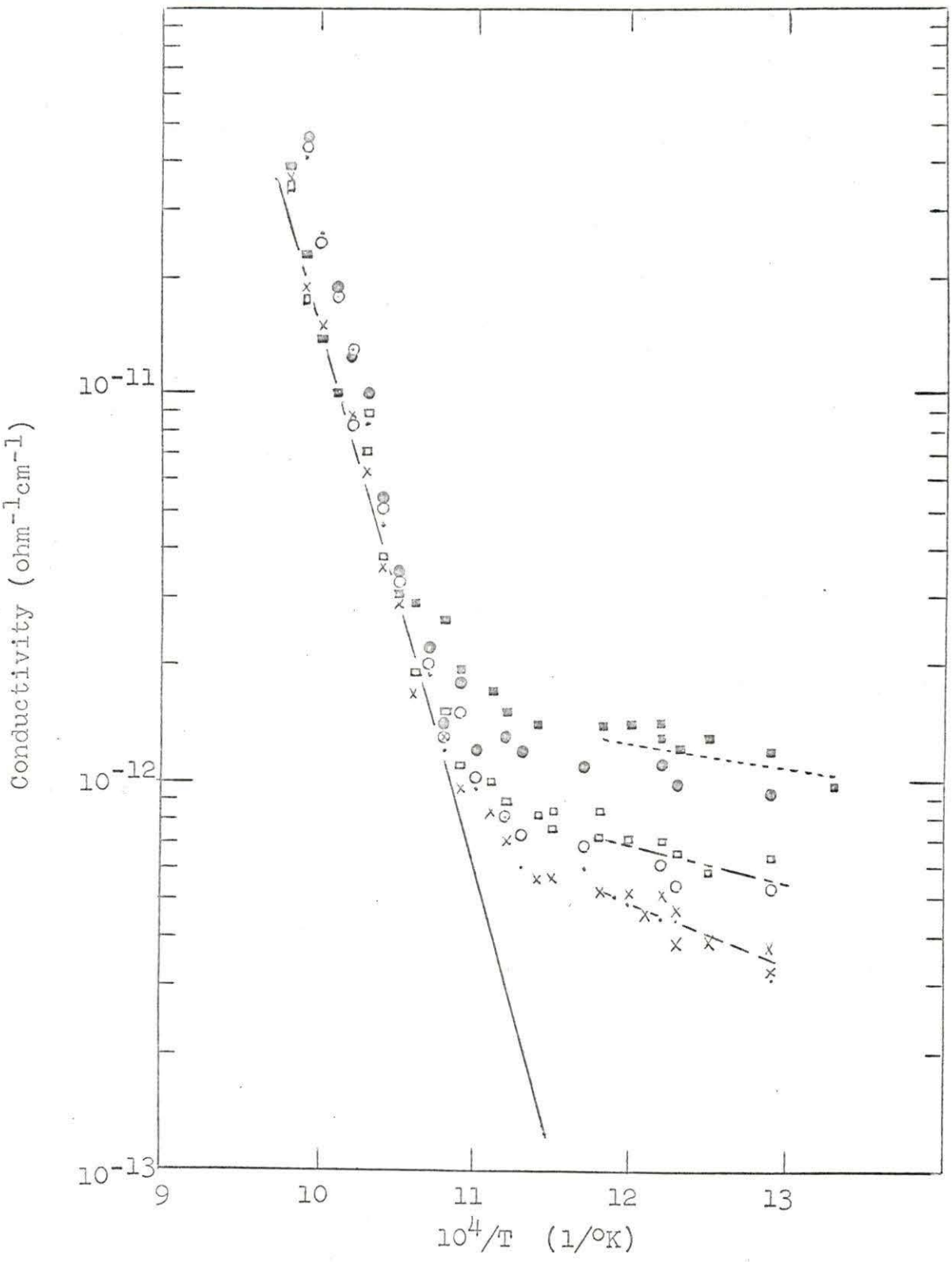
Conductivity (ohm^{-1}cm^{-1})
10^{-11}
10^{-12}
10^{-13}
9
10
11
12
13
$10^4/T$ (1/°K)

equal to the conductivity of the unirradiated specimen above 670° C. Similarly, there is a temperature below which radiation induced conductivity is clearly dominant and a function of both temperature and dose rate.

Figure 19 shows conductivity as a function of dose rate at a constant temperature of 550° C. This plot indicates that conductivity is not a linear function of dose rate. By plotting $\ln \sigma$ versus $\ln R$ it was found that a good fit was achieved for Equation 16. Values determined for a and c respectively were 1.11×10^{-15} $ohm^{-1}cm^{-1}$ and 0.734.

Continuing the assumption made earlier that the temperature dependency of radiation induced conductivity is exponential and noting visually that the data plots are roughly linear for each dose rate in the radiation effects region, a straight line was fitted for each dose rate. The values of F for these plots are, in order of increasing dose rate, 4.09×10^3 °K, 2.27×10^3 °K, and 1.71×10^3 °K. The inconsistency in these three values may be the result of experimental error. It may also suggest that carrier mobility in the radiation field is not an exponential function of reciprocal temperature. Further investigation, to include measurement of radiation induced conductivity at lower temperatures, would be required to better define the mobility term. The confidence level of the straight line fitting in Figure 19 was quite low; however, for the purpose of this

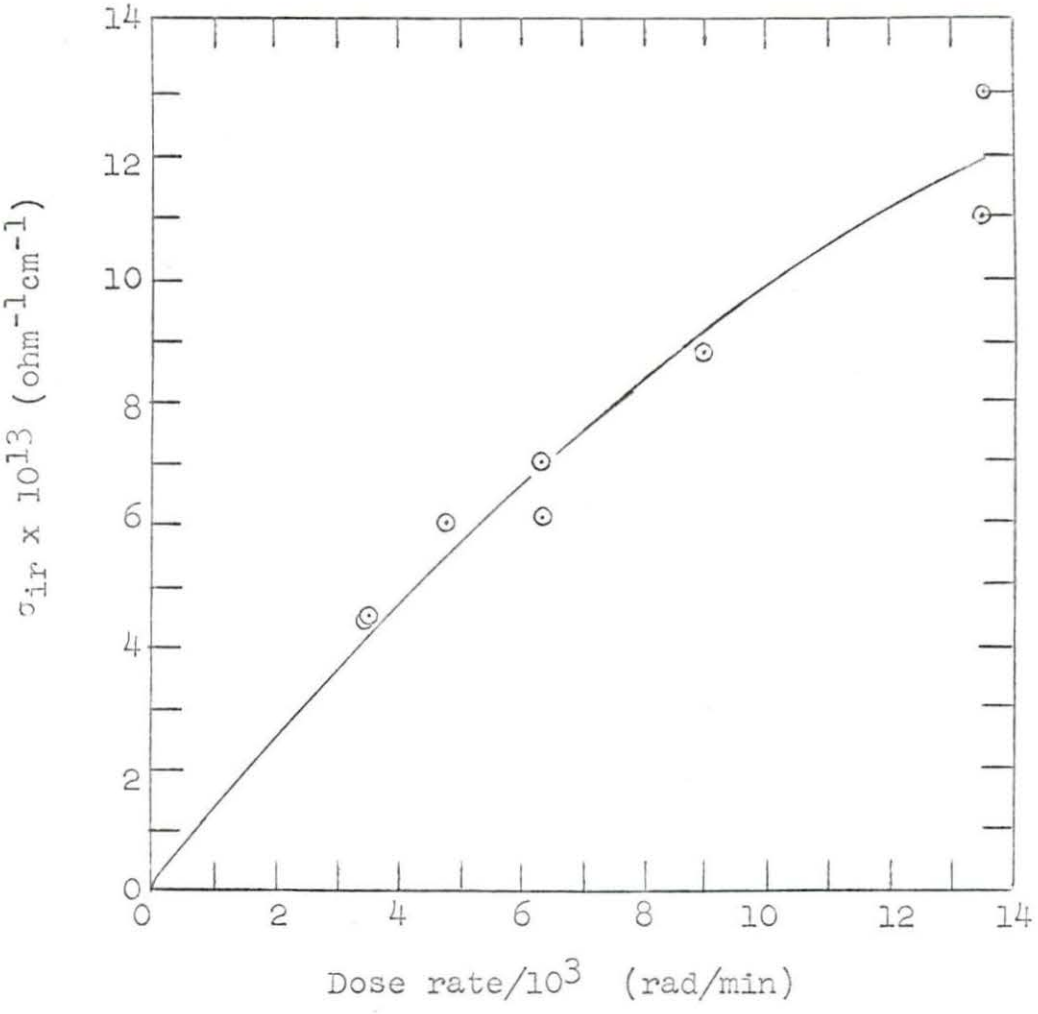

Figure 19. Dose rate dependency of radiation induced conductivity at 550° C

research exponential behavior was assumed and the middle value of 2.27×10^3 °K was selected as a good representative value for F in Equation 18. The value of b in Equation 18 was determined to be 1.73×10^{-14} $ohm^{-1}cm^{-1}$.

The results of a 30 minute test at the constant temperature of 600° C and a constant dose rate of 1.35×10^4 rad/min (a total dose of 4.04×10^5 rads) showed no detectable time dependency of the radiation induced conductivity. Thus the value of "n" in Equation 11 is zero for a period of 30 minutes or less. This result suggests that gamma radiation produced carriers are predominately "free" electrons elevated to the conduction band by the photoelectric and Compton effects. The production of nitrogen vacancies as reported by Khusidman (13) is apparently undectable at this low total dose and therefore is not a significant factor for a dose of 4×10^5 rads or less.

With all constants in Equation 18 now determined the expression for conductivity as a function of temperature and dose rate can now be written

$$\sigma = 1.99 \times 10^3 \, e^{-3.26 \times 10^4/T} + 1.73 \times 10^{-14} R^{0.734} e^{-2.27 \times 10^3/T} \quad (20)$$

SUMMARY AND CONCLUSION

The significant accomplishments of this research are summarized as follows:

1. An expression, Equation 20, has been determined which reflects the radiation effects on the electrical conductivity of pyrolytic boron nitride in the temperature range from 500° C to 750° C and a dose rate range from zero to 1.35×10^4 rads/min.

2. The thermal activation energy of the unirradiated specimen was determined to be 5.62 ev.

3. The dependency of conductivity on dose rate up to 1.35×10^4 rads/min was shown to be non-linear.

4. The conductivity was shown to be independent of time up to a total dose of 4×10^5 rads for the temperature and dose rates used in this experiment.

In conclusion it appears highly probable that pyrolytic boron nitride will be suitable for many dielectric and insulator applications in radiation fields comparable to dose rates studied in this research.

SUGGESTIONS FOR FURTHER WORK

Data obtained in this research was limited in accuracy by a fairly large background current resulting from radiation induced air conductance. An experiment is suggested that would provide refinement of the data reported herein by designing an apparatus which permits the introduction of the "hot" battery lead into the vacuum behind the radiation shield rather than in front of the shield as was done in this research. Further refinement might be achieved by designing a vacuum system with large diameter connections to the irradiation chamber, permitting achievement of a lower vacuum.

It is also suggested that an investigation be undertaken to determine the effects of a large gamma dose, on the order of 10^7 rads, on the electrical conductivity of pyrolytic boron nitride. The prospects of detecting a large dose effect is suggested by the work of Khusidman (13). Such an investigation would require long irradiation periods at high temperatures, therefore making necessary the provision for cooling of temperature sensitive parts of the apparatus.

TABLES

Table 1. Conductivity data for unirradiated specimen

Sample/ run	1/T $^{o}K^{-1}$ x 10^{-4}	I amperes x 10^{-10}	R ohms x 10^{10}	σ $ohm^{-1}cm^{-1}$ x 10^{-13}
1/1	12.1	.54	930	.34
1/1	11.8	1.4	360	.88
1/1	11.2	5.7	88	3.6
1/1	10.8	18	28	11
1/1	10.6	45	11	29
1/1	10.3	140	3.6	88
1/1	10.1	280	1.8	180
1/1	9.9	620	.81	390
1/2	12.6	.16	3600	.085
1/2	12.0	.77	650	.47
1/2	11.6	2.5	200	1.5
1/2	11.1	7.8	64	4.8
1/2	10.8	25	20	15
1/2	10.4	75	6.7	46
1/2	10.2	210	2.4	130
1/2	10.0	360	1.4	220
1/2	9.7	1200	.042	730
2/1	11.8	2.1	2400	.13
2/1	11.5	6.4	780	.41
2/1	11.2	2.5	200	1.6
2/1	10.9	6.2	81	3.9
2/1	10.6	18	28	11
2/1	10.4	46	11	29
2/1	10.1	125	4.0	79
2/1	9.9	310	1.6	200
2/1	9.8	450	1.1	290
2/2	11.7	.35	1400	.23
2/2	11.4	1.2	420	.76
2/2	11.1	3.7	140	2.3
2/2	10.8	10	50	6.4
2/2	10.5	27	19	17
2/2	10.3	20	7.1	45
2/2	10.0	190	2.6	120
2/2	9.6	680	.74	430

Table 2. Conductivity data for gamma dose of 3490 rad/min

Sample/ run	$1/T$ $^{o}K^{-1}$ x 10^{-4}	I amperes x 10^{-9}	R ohms x 10^{10}	σ $ohm^{-1}cm^{-1}$ x 10^{-13}
1/1	12.9	.50	100	3.1
1/1	12.2	.72	70	4.4
1/1	11.3	.99	51	6.0
1/1	11.0	1.6	32	9.6
1/1	10.8	2.0	25	12
1/1	10.5	4.9	10	31
1/1	10.3	14	3.7	83
1/1	10.1	29	1.7	180
1/1	9.9	68	.74	410
1/2	12.3	.72	70	4.4
1/2	11.7	.99	51	6.0
1/2	11.2	1.3	38	8.1
1/2	10.9	1.8	28	11
1/2	10.7	3.2	16	19
1/2	10.4	7.6	6.6	46
1/2	10.2	21	2.4	130
1/2	10.0	41	1.2	260
2/1	12.9	0.5	100	3.2
2/1	12.5	0.6	83	3.8
2/1	12.3	0.6	83	3.8
2/1	12.2	0.7	71	4.5
2/1	12.0	0.8	62	5.1
2/1	11.8	0.8	62	5.1
2/1	11.5	0.9	56	5.7
2/1	11.2	1.1	45	7.0
2/1	10.9	1.5	33	9.6
2/1	10.6	2.6	19	17
2/1	10.4	5.7	8.8	36
2/1	10.1	14	3.6	88
2/1	9.9	30	1.7	190

Table 2. (Continued)

Sample/ run	1/T $^{o}K^{-1}$ x 10^{-4}	I amperes x 10^{-9}	R ohms x 10^{10}	σ $ohm^{-1}cm^{-1}$ x 10^{-13}
2/2	12.9	0.6	83	3.8
2/2	12.5	0.6	83	3.8
2/2	12.3	0.7	71	4.5
2/2	12.2	0.8	62	5.1
2/2	12.0	0.8	62	5.1
2/2	11.8	0.8	62	5.1
2/2	11.5	0.9	56	5.7
2/2	11.4	0.9	56	5.7
2/2	11.1	1.3	38	8.4
2/2	10.8	2.0	25	13
2/2	10.5	4.4	11	29
2/2	10.3	10	5.0	63
2/2	10.0	25	2.0	160
2/2	9.8	56	.89	360

Table 3. Conductivity data for gamma dose of 6310 rad/min

Sample/ run	$1/T$ $^{o}K^{-1}$ x 10^{-4}	I amperes x 10^{-9}	R ohms x 10^{10}	σ $ohm^{-1}cm^{-1}$ x 10^{-13}
1/1	12.9	.87	58	5.3
1/1	12.2	1.0	50	6.1
1/1	11.3	1.2	42	7.3
1/1	11.0	1.6	31	9.9
1/1	10.8	2.1	24	13
1/1	10.5	5.2	9.6	32
1/1	10.3	14	3.6	85
1/1	10.1	30	1.7	180
1/1	9.9	69	.73	420
1/2	12.3	.87	58	5.3
1/2	11.7	1.1	45	6.8
1/2	11.2	1.3	38	8.1
1/2	10.9	2.4	21	15
1/2	10.7	3.3	15	20
1/2	10.4	8.2	6.1	50
1/2	10.2	21	2.4	130
1/2	10.0	42	1.2	250
2/1	12.3	1.0	50	6.3
2/1	12.2	1.1	45	7.0
2/1	11.8	1.3	38	8.4
2/1	11.5	1.3	38	8.4
2/1	11.2	1.4	36	8.8
2/1	10.9	1.8	28	11
2/1	10.6	2.9	17	19
2/1	10.4	5.9	8.5	37
2/1	10.1	14	3.6	88
2/1	9.9	30	1.7	190

Table 3. (Continued)

Sample/ run	$1/T$ $^{o}K^{-1}$ $\times 10^{-4}$	I amperes $\times 10^{-9}$	R ohms $\times 10^{10}$	σ $ohm^{-1}cm^{-1}$ $\times 10^{-13}$
2/2	12.9	1.0	50	6.3
2/2	12.5	0.9	54	5.8
2/2	12.2	1.0	50	6.3
2/2	12.0	1.1	45	7.1
2/2	11.8	1.1	45	7.1
2/2	11.5	1.2	42	7.6
2/2	11.4	1.3	39	8.1
2/2	11.1	1.6	31	10
2/2	10.8	2.4	21	15
2/2	10.5	4.8	10	32
2/2	10.3	11	4.5	71
2/2	10.0	26	1.9	170
2/2	9.8	57	.88	360

Table 4. Conductivity data for gamma dose of 13500 rad/min

Sample/ run	$1/T$ $^{o}K^{-1}$ x 10^{-4}	I amperes x 10^{-9}	R ohms x 10^{10}	σ $ohm^{-1}cm^{-1}$ x 10^{-13}
1/1	12.9	1.5	33	9.3
1/1	12.2	1.7	29	11
1/1	11.3	2.0	25	12
1/1	11.0	2.0	25	12
1/1	10.8	2.4	21	15
1/1	10.5	5.6	8.9	34
1/1	10.3	16	3.1	99
1/1	10.1	31	1.6	190
1/1	9.9	71	.70	440
1/2	12.3	1.6	27	9.9
1/2	11.7	1.8	28	11
1/2	11.2	2.2	23	13
1/2	10.9	3.0	17	18
1/2	10.7	3.6	14	22
1/2	10.4	8.6	5.8	53
1/2	10.2	22	2.3	130
1/2	10.0	43	1.2	260
2/1	12.3	1.9	26	12
2/1	12.2	2.1	24	13
2/1	11.8	2.3	22	14
2/1	11.4	2.3	22	14
2/1	11.1	2.6	19	17
2/1	10.8	4.2	12	26
2/1	10.5	5.1	9.8	31
2/1	10.3	10	5.0	63
2/1	10.0	23	2.2	140
2/1	9.8	58	.86	370

Table 4. (Continued)

Sample/ run	$1/T$ $^{o}K^{-1}$ $\times 10^{-4}$	I amperes $\times 10^{-9}$	R ohms $\times 10^{10}$	σ $ohm^{-1}cm^{-1}$ $\times 10^{-13}$
2/2	13.3	1.5	33	9.6
2/2	12.9	1.9	26	12
2/2	12.5	2.0	25	13
2/2	12.2	2.1	23	14
2/2	12.0	2.2	23	14
2/2	11.8	2.2	23	14
2/2	11.2	2.4	21	15
2/2	10.9	3.0	17	19
2/2	10.6	4.5	11	29
2/2	10.4	7.7	6.5	49
2/2	10.1	1.6	3.1	100
2/2	9.9	37	1.4	230

Table 5. Data for determination of dose rate dependency of conductivity at 550° C

Sample	Dose rate rad/min x 10^{3}	I amperes x 10^{-9}	R ohms x 10^{10}	σ $ohm^{-1}cm^{-1}$ x 10^{-13}
1	3.49	.72	71	4.5
1	6.31	1.0	50	6.1
1	13.50	1.7	29	11
2	3.49	.72	71	4.5
2	4.75	.95	53	6.0
2	6.31	1.1	45	7.0
2	8.95	1.4	36	8.8
2	13.50	2.1	24	13

Table 6. Background current data for irradiated apparatus without specimen

$1/T$ $^{o}K^{-1}$ x 10^{-4}	I^{a} amperes x 10^{-10}	I^{b} amperes x 10^{-10}	I^{c} amperes x 10^{-10}
12.9	3.8	7.2	9.1
12.4	3.8	7.4	9.1
12.2	3.8	7.4	9.2
11.8	3.9	7.5	9.3
11.5	4.1	7.7	9.6
11.2	4.4	7.9	9.9
11.1	4.3	8.2	10.2
10.9	4.3	8.2	10.4
10.8	4.4	8.5	10.5
10.6	4.4	8.5	11.0
10.4	4.8	9.1	11.2
10.3	5.0	9.5	11.8
10.1	5.2	9.6	12.2
10.0	5.7	10.2	13.0
9.7	6.5	11.4	14.4

[a]Gamma dose rate of 3.49×10^{3} rad/min.

[b]Gamma dose rate of 6.31×10^{3} rad/min.

[c]Gamma dose rate of 1.35×10^{4} rad/min.

ERROR ANALYSIS RESULTS

The uncertainty in the single values of conductivity due to measuring apparatus error and specimen dimensional variation is 5.6 percent.

The confidence levels of the straight line least square fit of specimen conductivities for condition indicated are

Unirradiated	95%
3.49×10^3 rad/min	86%
6.31×10^3 rad/min	56%
1.35×10^4 rad/min	33%

The uncertainties of the mean conductivity values corresponding to the straight line least square fit for the unirradiated specimens are 91 percent for values in the 10^{-14} $ohm^{-1}cm^{-1}$ range and 38 percent for all other values.

The uncertainties for mean conductivity values of irradiated specimens are

3.49×10^3 rad/min	11%
6.31×10^3 rad/min	9%
1.35×10^4 rad/min	12%

BIBLIOGRAPHY

1. Basche, M. and Schiff, D. New pyrolytic boron nitride. Mat. in Des. Eng. 59, No. 2: 78-81. 1964.

2. Westinghouse Electric Corporation. Developing a high temperature capacitor. Westinghouse R and D Letter. Pittsburgh, Pa., Westinghouse Electric Corporation. February 1968.

3. Union Carbide Corporation, Carbon Products Division. BORALLOY boron nitride. Union Carbide Corporation, Carbon Products Division Tech. Info. Bul. No. 713-204EF. ca. 1964.

4. Bogoroditskii, N. P. and Pasynkov, V. V. Radio and electronics materials. London, Iliffe Books Ltd. 1967.

5. Azaroff, V. L. and Brophy, J. J. Electronic processes in materials. New York, N.Y., McGraw-Hill Book Co., Inc. c1963.

6. Adler, R. B., Smith, A. C. and Longini, R. L. Introduction to semiconductor physics. New York, N.Y., John Wiley and Sons, Inc. c1964.

7. Ioffe, A. F. Physics of semiconductors. New York, N.Y., Academic Press Inc. c1960.

8. Kittel, C. Elementary solid state physics: a short course. New York, N.Y., John Wiley and Sons, Inc. c1962.

9. Dekker, A. J. Solid state physics. Englewood Cliffs, N.J., Prentice-Hall, Inc. 1960.

10. Jones, D. C., Reid, F. J., Chapin, W. E., Hamman, D. J. and Wyler, E. N. Transient radiation effects on electronic components and semi-conductor devices. Battelle Memorial Institute Radiation Effects Information Center Report No. 26. 1963.

11. Vul, B. M. The effect of gamma radiation on the electrical conductivity of insulators. Sov. Phys.-Sol. St. 3: 1644-1650. 1962.

12. Drennan, J. E. and Hamman, D. J. Space-radiation damage to electronic components and materials. Battelle Memorial Institute Radiation Effects Information Center Report No. 39. 1966.

13. Khusidman, M. B. and Sharupin, B. N. Investigation of irradiated boron nitride by electron paramagnetic resonance. Radiokhimiya 9: 279-280. 1967. Original available nut not translated; abstracted in Nuc. Sci. Abs. 21: 35993. 1967.

14. Khusidman, M. B. and Neshpar, V. S. F centers in hexagonal boron nitride enriched with B^{10} isotope. Sov. Phys.-Sol. St. 10: 975-976. 1968.

15. Dau, G. J. and Davis, M. V. Gamma-induced electrical conductivity in alumina. Nuc. Sci. and Eng. 25: 223-226. 1966.

16. Peters, D. W., Feinstein, L. and Peltzer, C. On the high-temperature electrical conductivity of alumina. J. of Chem. Phys. 42: 2345-2346. 1965.

17. Cohen, J. Electrical conductivity of alumina. Am. Cer. Soc. Bul. 38: 441-446. 1959.

18. Dau, G. J. and Davis, M. V. Electrical conductivity of alumina at temperatures in a reactor environment. Nuc. Sci. and Eng. 21: 30-33. 1964.

19. D-C resistance or conductance of insulating materials. Am. Soc. for Test. and Mat. 1969 Book of ASTM Standards, Part 29: 181-203. c1969.

20. Carlson, Michael C. J. The effect of gamma radiation on the conductivity of sodium chloride. Unpublished Ph.D. thesis. Ames, Iowa, Library, Iowa State University. 1968.

21. Matsumura, T. Electrical properties of alumina at high temperature. Can. J. of Phys. 44: 1685-1698. 1966.

22. Radiation-effects state of the art 1965-1966. Battelle Memorial Institute Radiation Effects Information Center Report No. 42. 1966.

ACKNOWLEDGEMENTS

I would like to thank Dr. Glenn Murphy for making funds available to conduct this research.

I would like to thank Dr. Michael C. J. Carlson for the many hours of consultation and assistance provided me and for the many helpful suggestions he gave in helping me complete this work.

Finally, I would like to thank Terry McConnell and Dean Flack of the Electrical Engineering Shop for the skillful and professional job done in fabricating the equipment that made completion of this thesis possible.